ACS APPLIED POLYMER MATERIALS

pubs.acs.org/acsapm Article

Low-Isocyanate Polyurethane Foams with Improved Stability and Compression Modulus Prepared from Biosourced and Landfill-Diverted Materials

Rebecca Mort, Erin Peters, Elizabeth Griffin, Greg Curtzwiler, Keith Vorst,* and Shan Jiang*

Cite This: https://doi.org/10.1021/acsapm.3c01536

ABSTRACT: Polyurethane foams are widely used in a variety of applications that impact everyday life, including single-use packaging and durable furniture. Currently, the industry depends primarily on petroleum-based reactants, such as polyols and isocyanates. Isocyanates are particularly troublesome due to their harmful effects on human health but are also crucial for achieving foam properties, such as rigidity. In this study, we demonstrate that cost-competitive, scalable, and more sustainable foams can be attained using biobased polyol substitutes along with landfill-diverted biofillers (rice hulls and coffee chaff) at a lower ratio of isocyanate. To avoid the common collapsing issue, we designed a prepolymerization step that can consistently produce high-quality foam with zero volume loss after expansion. The addition of biofiller increased the foam compression modulus drastically up to 400% at the same isocyanate concentration. Therefore, the incorporation of the biofiller provided a mechanism to enhance the mechanical properties without increasing the amount of isocyanates. Additionally, the reproducibility and foam properties can be further improved through grinding and sieving. The finer particles can be loaded at even higher levels without negatively impacting the mechanical properties. The same approach can be expanded to other types of biobased cellulosic biofillers. The results put forward a scalable, economical, and more sustainable route to improve foam performance while reducing isocyanate usage by incorporating biobased content.

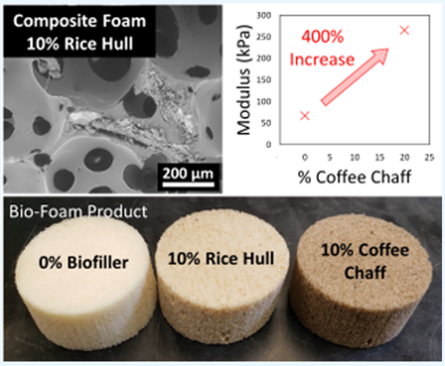

KEYWORDS: *biofoam, low isocyanate, landfill diversion, rice hull, coffee chaff*

■ INTRODUCTION

Polyurethane foams play a vital role in daily life. These foams are formulated to possess a wide range of stiffness, density, and durability to meet the requirements of a multitude of applications such as packaging, furniture cushions, and building insulation. However, the production of polyurethane foams involves the use of toxic chemicals which can cause potentially life-threatening respiratory damage in workers who experience long-term exposure.[1,2] At the end life of these products, disposal of foams in landfills is the status quo. Of all polyurethane postconsumer landfill waste, flexible foams and rigid foams account for 46 and 22%, respectively.[3] With the growing necessity for more sustainable materials and the safety concerns associated with manufacturing, there is an urgent need to develop greener alternatives that can quickly be adopted by the industry.[4,5]

Sourcing raw materials from plants and agricultural waste could offer a more sustainable path for polyurethane-based foams. The chemicals traditionally used to formulate polyurethane foams are primarily derived from nonrenewable petroleum sources. Previous studies have explored replacing traditional petroleum-based polyols with various modified plant oils[6−8] and many have successfully produced rigid and flexible polyurethane foams. However, they still suffer from limitations such as slower reaction speeds. Additionally, most plant oils do not naturally contain the hydroxyl groups that are required for polymerization, resulting in the need for chemical modification.[9,10] Castor oil (CO) is one of the exceptions; it naturally has an average −OH functionality of 3, making it possible to form a cross-linked polymer without any prior modification.[11−13] Methods for overcoming limitations with reaction kinetics in plant oil polyols have also been explored.[14,15] Therefore, CO is a particularly promising polyol alternative.

Reducing isocyanate concentrations in foam formulations increases safety and lowers cost. Isocyanates are toxic chemicals that irritate mucous membranes, resulting in severe and chronic asthma symptoms in individuals who have prolonged exposure, in some cases resulting in death.[1,2] However, the current isocyanate alternatives cannot fully

Received: July 10, 2023
Accepted: July 25, 2023

meet the requirements for industrial free-rise foams and it is not possible to completely eliminate the use of isocyanate altogether.[16−18] Therefore, it is important to explore methods for reducing the amount of isocyanates used in foam production which can be immediately implemented in industry, while isocyanate replacement research is ongoing.

Isocyanate selection and ratio are crucial factors for determining polymer and foam properties such as rigidity.[19] Because durable and short-term-use goods require a wide range of properties for different applications, any method to reduce isocyanates must still possess the range of desired physical properties. In past studies, blending in a particulate phase to form a composite structure has been a popular approach for altering foam properties. Nanoclay particles and crystalline nanocellulose in particular have been used to increase foam compression strength.[20,21] The downside of such composites is the added cost and sometimes limited availability of highly refined particles, which can become prohibitive for large-scale manufacturing.

To address these issues, we have developed a simple method to produce castor-oil-based polyurethane composite foams made with ground rice hulls (RH) and coffee chaff (CC) as the particle phase. RH and CC are agricultural byproducts currently disposed primarily in landfill. Because they are considered waste, using these materials as a filler not only diverts them from landfill but can also be cost-effective with prices ranging from \$5 to \$10 per ton (0.2−0.5 cents per pound).[22] In addition, RH and CC also have the benefit of having hydroxyl groups on the particle surfaces that are reactive with isocyanates, thereby strengthening the interface of the composite. Successful incorporation of RH and CC within the polyurethane foam matrix provides the proof of concept of utilizing many other cellulosic biomass waste materials such as corn stover and wheat husk. Diversifying the sources of biomass used for biofillers would prove to be both economically and environmentally beneficial.

Previous studies have shown the use of cellulosic additives within polyurethanes.[23−25] Ghasemi et al. produced foams containing cellulose nanofilbrils with increased tear resistance and compressive stiffness at loading as low as 0.1%.[24] Though this clearly demonstrates that nanofibrils are effective at improving performance, such additives have disadvantages of high cost, extensive processing, and difficult handling compared to ground RH and CC. Zhang et al. were able to incorporate various biomass particles including rapeseed straw and rice straw into rigid foams with high isocyanate index (1.5).[25] Their results demonstrated that higher particle loads could be detrimental to structural stability during foaming, leading to partial collapse. Further questions remained regarding the underlying mechanisms relating different filler types to differences in foam properties.[25] To address these challenges, we have developed a robust methodology for consistently producing composite foams with low isocyanate index, 100% biobased castor oil, and particle loading up to 30 wt %. We further explored the effects of particle type and grinding on the foam properties. In this way, we met our goals to produce foams with a wide range of mechanical properties and to produce a low isocyanate foam with mechanical strength competitive with a higher isocyanate index foam.

A series of formulations were developed with both RH and CC biofillers, loaded up to 30 wt %, while keeping all other components, including isocyanate index, the same. Challenges with foam stability were encountered in the early stages of the formulation development. After expansion, while the foams remained tacky, the foam cells would begin to collapse, causing volume loss. The polymer films were not stable enough to withstand negative pressure within the outer cells produced by the temperature gradient of the cooling foam. Previous works with biobased polyols have described a similar phenomenon.[14] Researchers have resolved reaction kinetics issues in the past by chemically modifying CO or by mixing plant oils with other polyols.[14,15] For this study, we mitigated the collapsing issue in our subsequent formulations through the addition of a prepolymerization step and elevated curing temperatures. As a result, all samples prepared for this study had a zero volume loss after expansion.

Previously, we studied these biofillers in an extruded foam system that also showed increased mechanical strength, although the detailed mechanism was not thoroughly investigated.[26] It was hypothesized that the addition of biofiller particles would increase the rigidity of otherwise flexible castor oil foams due to a combination of strong interaction with the polymer matrix through covalent bonding and the formation of a well-dispersed reinforcing particle network within the foam cell walls. Mechanical and thermal properties were compared across the formulations to determine: (1) how significantly biofillers affect foam stiffness, (2) what property trade-offs could exist, and (3) if the biofiller type (RH vs CC) influences realized properties. In assessing the performance of these composite foams, ANOVA statistical analysis was performed to identify samples/categories that exhibited statistically significant differences. Practical differences were also considered, as variability in some quantitative data could cause statistical analysis to "overlook" differences that may still be meaningful in real-world applications. Preliminary experiments determined that some of the formulations yielded highly varied results. Therefore, we explored additional factors such as grinding.[27,28] The original particle grinds contained a wide size and shape distribution with some particles as large as 800−900 μm. To determine if foam properties could be made more consistent by controlling the particles, we prepared a more finely ground rice hull (FRH) filler and incorporated it into another series of formulations.

The biofiller foams showed statistically significant increases in mechanical strength with up to 400% increases in the compression modulus. The comparison of RH and FRH foams also suggested that the particle size can be used to control foam properties and reproducibility. Overall, the results of this study demonstrate the use of RH and CC biofillers as a promising and economically viable means to alter biobased polyurethane foam properties without a need to increase the isocyanate index.

EXPERIMENTAL SECTION

For polyurethane synthesis, research-grade castor oil, liquid synthesis-grade 4,4′-metheylenediphenyl diisocyanate (MDI), and hexamethey-lene diisocyanate (HDI) were obtained from Sigma-Aldrich (St. Louis, MO). Dibutyltin dilaurate (>95% purity) from TCI America (Portland, OR) was used as a catalyst. A silicone surfactant, VORASURF DC 2584, was provided by Dow Chemical (Midland, MI). Biofiller materials, coffee chaff, and rice hulls were obtained from a commercial source. Deionized water was used as a chemical blowing agent.

Coffee chaff and rice hulls were ground separately in a cyclone mill to produce biofiller particles. The ground material was sieved through a 350 μm mesh, and the coarser media was returned to the mill for further size reduction. To test the impact of particle size distribution,

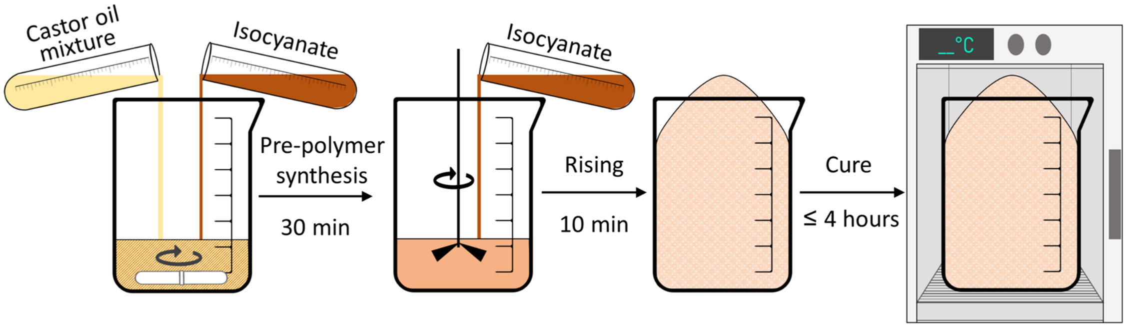

Figure 1. Schematic plot of the foam synthesis process.

a finer grind of rice hulls was produced using the same method with a 150 μm sieve. Due to limitations in available material at the time this study was conducted, there was an insufficient amount of coffee chaff to prepare both the regular and fine grind for direct comparison. Given the nature of the biofiller materials and their sourcing, heterogeneity is to be expected with regard to the particle properties. The ground dry particles had average apparent densities of 0.389, 0.528, and 0.438 g/cm^3 for coffee chaff, rice hull, and fine rice hull, respectively. Detailed characterization of particle size and shape properties is provided in the Results and Discussion section.

Composite polyurethane foams were synthesized in a three-step process: (1) preparation of a prepolymer containing castor oil and biofiller particles partially reacted with isocyanate, (2) reacting the prepolymer with additional isocyanate and water to form a free-rise foam, and (3) curing fully expanded foams in an oven set to a temperature approximately 5 °C above the maximum reaction temperature. Figure 1 shows a schematic outlining the foam synthesis process. Tables 1 and 2 show the ratios of all components. Isocyanate index (NCO index) was calculated as a ratio of all −NCO groups to all −OH groups (from castor oil and water). This calculation does not include potential −OH groups present (confirmed with infrared spectroscopy, see the Results and Discussion section) on biofiller particle surfaces because, though the particles are generally cellulosic and have −OH groups available, the degree of reactivity is difficult to predict and could vary depending on particle type, size, and shape. Therefore, though all samples, with one exception, had the same total equivalents of isocyanates, the true NCO index for samples containing biofillers may be lower than 0.75. One additional formulation with 0% biofiller and a 1.0 NCO index was included in this study for a comparison of mechanical properties. The 1.0 NCO index foam was prepared with the same HDI:MDI ratio as the 0.75 NCO index foams.

Table 1. Reactant Amounts Of All Nonisocyanate Components in Castor Oil Polyurethane Foams[a]

formulation component (nonisocyanates)	weight % relative to castor oil
biofiller	0−30% (formulation-dependent)
surfactant	1%
catalyst	0.5%
blowing agent	5%

[a] Amounts are measured relative to the mass of castor oil to maintain consistent ratios.

Table 2. Reactant Amounts of All Isocyanate Components in Castor Oil Polyurethane Foams[a]

formulation component (isocyanates)	isocyanate index	% used in prepolymer	% used in foaming step
HDI	0.3	33	67
MDI	0.45	11	89
total	0.75	20	80

[a] Amounts are calculated by a target isocyanate index with a certain percentage of each isocyanate used in the prepolymer step and the remaining used in the foaming step.

The prepolymer was prepared by mixing the appropriate amount of castor oil, biofiller, surfactant, and catalyst with a magnetic stir bar until homogeneous (approximately 5 min). A portion of the HDI and MDI was then added, and the subsequent reaction was allowed to proceed at room temperature while stirring constantly (approximately 60 rpm) for 30 min. After 30 min, the completed prepolymer was removed from the stir plate.

The foaming reaction was completed by first adding the water to the prepolymer and mixing vigorously for about 30 s. The remaining HDI and MDI were then added and mixed for another 30 s until homogeneous. The foam was allowed to expand at room temperature for at least 10 min. After expansion, the foam, still inside the mold, was placed in an oven to cure until samples could be removed from the mold without damage or shrinkage (up to 4 h). The curing temperature was determined for each formulation by measuring the maximum reaction temperature during expansion with a thermocouple placed in the center of the sample.

The prepolymers were characterized immediately after the 30 min reaction was completed using Fourier transform infrared spectroscopy (Thermo Nicolet 6700 FT-IR with a diamond Golden Gate ATR). Each spectrum collection consisted of 32 scans done with a DTGS detector with a 2 cm^{-1} resolution. ATR-FTIR (with the same scanning parameters) was used to analyze the ground biofiller particles alone and biofiller particles mixed with MDI in a 1:1 volume ratio and 1 wt % catalyst. The particle/MDI mixtures were mixed on a stir plate for approximately 15 min prior to the first scan. They were returned to the stir plate to continue the reaction and scanned again after 30 and 60 min. The mixture was kept under an inert gas atmosphere.

Gel permeation chromatography (Agilent 1200 HPLC with a refractive index detector) was used to determine chain growth in the prepolymers. All samples were dissolved in HPLC grade tetrahydrofuran (THF) at a concentration of 2 mg/mL and then filtered with 0.45 μm PFTE filters. Since the biofiller particles were not soluble, all biofiller and any castor oil species attached to the particles were removed during filtration. 100 μL of each sample was injected into the columns (Agilent PL1110-6504 and PL1110-6515) with THF at a flow rate of 1 mL/min. The GPC data was analyzed using ASTRA 8.0.2.5 software (Wyatt Technologies, Santa Barbara, CA).

Foam samples were characterized by scanning electron microscopy (SEM). Samples were prepared by cutting the cross section perpendicular to the rising direction and then sputter coated with iridium. An FEI Quanta-FEG 250 SEM instrument with a 1 nm resolution operating at an accelerating voltage of 10 kV was used in variable pressure mode. The SEM images were analyzed with ImageJ software (U.S. National Institutes of Health, Bethesda, MD) to measure the cell size (maximum Feret length). 50 cells were measured for each sample.

The density of the foam samples was determined by cutting the samples into cylinders with 2 in. diameter and 1 in. height. The mass of the samples was measured using a precision balance with a

https://doi.org/10.1021/acsapm.3c01536
ACS Appl. Polym. Mater. XXXX, XXX, XXX−XXX

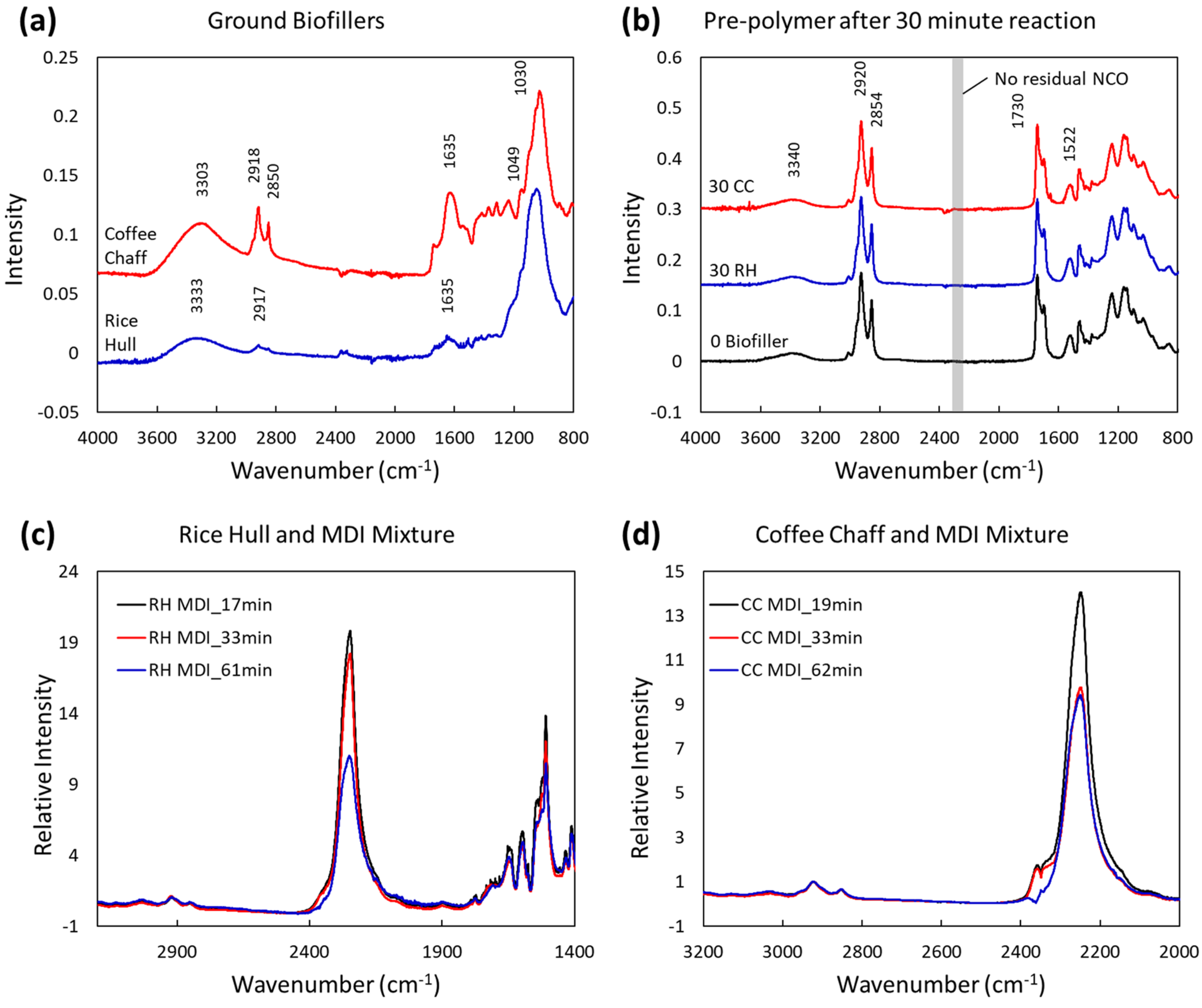

Figure 2. FT-IR spectra for (a) ground biofiller particles, (b) prepolymers containing no biofiller, 30% CC, and 30% RH after a 30 min reaction, (c) rice hull particles mixed with isocyanate and scanned at three time intervals, and (d) coffee chaff particles mixed with isocyanate and scanned at three time intervals. In (c) and (d), the biofiller particles were mixed with MDI in a 1:1 volume ratio and 1 wt % catalyst.

resolution of 0.1 mg (SI-234, Denver Instrument, Bohemia, NY). Density was calculated by dividing the mass by the sample volume. These same cylindrical samples were subsequently used for the thermal conductivity and then compression modulus characterization.

The thermal conductivity of the foam samples was measured with a Hot Disk TPS 1500 (Hot Disk Instruments, Göteborg, Sweden) with a Kapton sensor. Three sets of replicates for each foam formulation were tested, and an average value was calculated. All thermal conductivity tests were conducted at room temperature.

Compression testing was conducted by using an Autograph AGS-J (Shimadzu Corp., Kyoto, Japan) universal electromechanical tester with a 5 kN load cell. The procedure followed ASTM D3574-17 Test C.[29] The sample was placed on the lower compression platen, and the upper platen was lowered until a force of 1 N was registered. The distance between the platens at this point was set as 0% strain. The sample was then compressed to 50% strain at a constant rate of 50 mm/min. The sample was held at 50% strain for 1 min before returning to the original position. Samples were oriented such that force was always applied parallel to the foam rising directions. Compression modulus was calculated from the initial slope of the stress−strain curves. At least 5 replicate samples were tested for each foam formulation.

Cyclic creep recovery tests were conducted on the foam samples to characterize differences in viscoelasticity and fatigue behavior. Samples were cut into cubes measuring 10 mm^3 and then loaded into a DMA 7e (PerkinElmer, Waltham, MA) with a parallel compression plate fixture. All experiments were isothermal with the furnace set to 25 °C. At the start of the test, the sample was held under a static force of 10 mN for 1 min, after which the first cycle began. In each cycle, a creep force of 1000 mN was applied for 1 min followed by a recovery force of 10 mN for 2 min. Each test consisted of 20 cycles. Again, samples were oriented such that force was always applied parallel to the foam rising directions.

Optical images of the ground biofiller particles were taken by using a 3D Surface Profiler VK-X1000 microscope (Keyence Corporation of America, Itasca, IL) with 5× and 10× magnification lenses. Additionally, particle size and shape distributions were characterized with a Solidsizer dynamic image analysis system (JM Canty, Lockport, NY). The Solidsizer uses a high-speed camera to capture images of individual backlit particles as they fall off a vibrating platform at a controlled rate. The camera had a calibrated resolution of 6.2 μm/pixel. Area, perimeter, and Feret length data were gathered from each image to calculate the area equivalent diameter, aspect ratio (AR), and elliptical form factor (EFF). Area equivalent diameter is the diameter of a sphere with the same cross-sectional area as that of the particle.

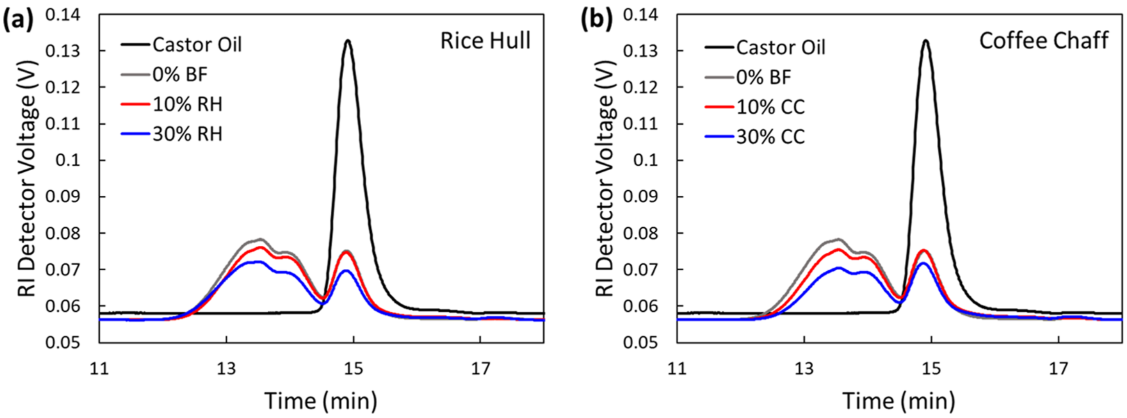

Figure 3. GPC chromatograms of prepolymers containing (a) rice hulls and (b) coffee chaff. Castor oil and 0% biofiller prepolymer are displayed for comparison. All samples were dissolved in tetrahydrofuran and filtered to remove insoluble material (biofiller particles).

AR is a ratio of the minimum Feret length to the perpendicular length. EFF is a ratio of the perimeter of a theoretical ellipse with equivalent area and aspect ratio to the actual particle perimeter.[30]

Statistical analysis of data sets with multiple data points per sample/category was conducted using JMP Pro 16, SAS Institute, Inc., Cary, NC. Statistically significant differences between samples were identified through one-way ANOVA and post hoc *t* tests with a 0.05 alpha value.

■ RESULTS AND DISCUSSION

Free-rise composite polyurethane foams were produced using castor oil, a mixture of isocyanates including hexamethylene diisocyanate (HDI) and methylenediphenyl diisocyanate (MDI), and ground biofiller particles. HDI was selected to provide more flexibility, while the benzene ring structures present in MDI are comparatively more rigid. Castor oil contains 3 secondary hydroxyl groups which grant the capability of polymer branching and cross-linking. Initial formulation testing suggested that the castor oil reaction speed was a limiting factor. If polymerization and blowing reactions were performed simultaneously without any prior steps, bubbles would nucleate and quickly coalesce into large voids or collapse as there was insufficient polymer growth and curing to form stable cells. Several factors impact the polyol reactivity and reaction kinetics. Castor is likely limited by the fact that all hydroxyl groups are secondary, which are generally known to be less reactive than primary groups.[31] Formulations can be adjusted to compensate for limited reactivity through catalyst selection.[32,33] For this reason, a tin-based catalyst known to promote the polymerization reaction over the blowing reaction was selected.[34]

As a result of these reaction challenges, a prepolymer step was added before foaming, which plays a critical role in foaming properly and reproducibly. In this step, castor oil was partially reacted with a small amount of isocyanate to begin the process of building the polymer without needing to compete with a blowing agent. Therefore, when the blowing agent was introduced in the foaming step, the polymerization reaction was effectively given a "head start", providing a more optimal balance between the two reactions. The prepolymer, consisting of oligomeric castor oil species along with some residual unreacted castor oil, was shelf stable and increased the stability of the expanding foams. Infrared spectroscopy was employed to both confirm the reactive groups present in the prepolymer and to analyze the biofiller particles.

Figure 2 displays representative FT-IR spectra for biofiller particles and prepolymers wherein the data demonstrate the presence of hydroxyl groups in both biofiller particle types and the completion of the reaction in all prepolymers regardless of particle content. The particles alone were analyzed to confirm the presence of molecular characteristics typical of cellulosic materials. Both rice hulls and coffee chaff have similar spectra. The broad peak between 3600 and 3000 cm^{-1} can be attributed to hydroxyl groups.[35,36] The peaks at 2918 cm^{-1} (in both) and 2850 cm^{-1} (in CC) can be attributed to methyl and methylene groups, respectively.[35,37] Both have peaks at 1635 cm^{-1} which indicate alkene groups and possibly −OH bending from adsorbed water molecules.[37,38] The peaks at 1030 cm^{-1} (CC) and 1049 cm^{-1} (RH) indicate carbonyl stretching.[35,37,38]

Prepolymer samples were analyzed with FT-IR immediately after the 30 min prepolymer reaction was completed, with representative spectra displayed in Figure 2b. No discernible differences between the spectra were observed across all samples and replicates. Therefore, interactions between biofiller particles and the prepolymer cannot be differentiated from the prepolymer itself using FTIR characterization. The peaks present are characteristic of castor oil and potential polyurethane linkages.[36,39] The broad band between 3600 and 3200 cm^{-1} can be attributed mainly to hydroxyl groups, though this region also overlaps with 3344 cm^{-1} which is associated with amide groups. The peak at 1730 cm^{-1} indicates stretching of carbonyl groups, and the peak at 1522 cm^{-1} indicates C−N bending in urethane linkages. It is important to note the lack of any peak in the range attributed to −NCO groups (2248 cm^{-1}). Thus, there is no unreacted isocyanate remaining after the 30 min prepolymer reaction.

Given the confirmed presence of −OH groups in the biofiller particles, it was hypothesized that the particles could react with isocyanate molecules, thus, forming covalent bonds between the particles and the rest of the polymer matrix. Therefore, particles were mixed with an isocyanate and catalyst to observe if the isocyanate reacted over time. Figure 2c,d shows the FTIR spectra for the particle-isocyanate mixtures at 3 time points (approximately 15, 30, and 60 min). The curves were all normalized relative to the peak at 2918 cm^{-1}. The peak at 2248 cm^{-1} corresponds to NCO groups.[39] The rice hull particles show a small decrease in the isocyanate peak between 17 and 33 min followed by a decrease of nearly 50% after 61 min. In comparison, the coffee chaff particles show a decrease of about 30% between 19 and 33 min after which it

https://doi.org/10.1021/acsapm.3c01536
ACS Appl. Polym. Mater. XXXX, XXX, XXX−XXX

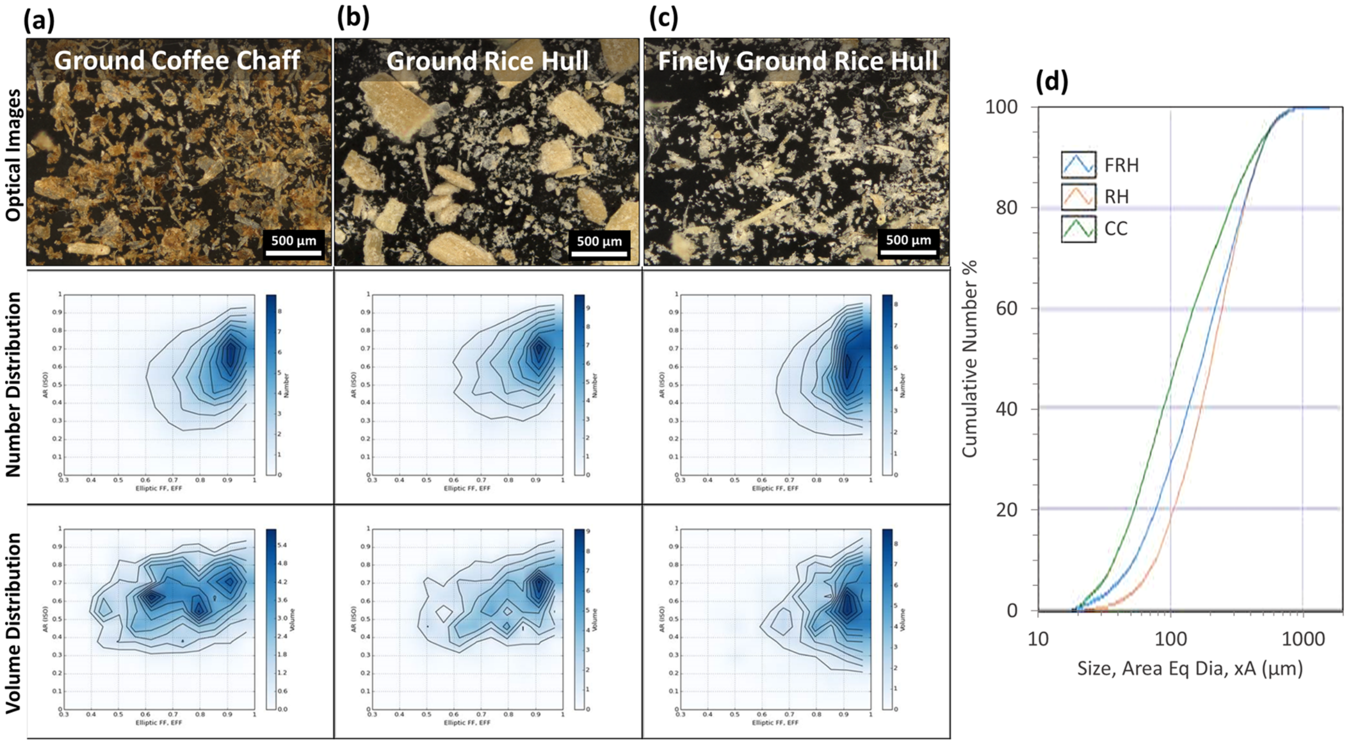

Figure 4. Biofiller particle shape and size characteristics. (a−c) Optical images of particles (top), particle shape maps shown in number distribution (middle), and volume distribution (bottom). Each particle type is represented as (a) coffee chaff, (b) rice hull, and (c) fine rice hull. Size data is displayed as (d) particle size distribution by cumulative number percentage. Size is given as an area equivalent diameter. Average particle sizes are 50 μm (fine rice hull), 136 μm (rice hull), and 86 μm (coffee chaff).

remains essentially constant. The decreases in the NCO peak clearly indicate the isocyanate is reacting, and given that all particle-isocyanate mixtures were prepared and held under an inert gas atmosphere, it is highly unlikely that the reaction is occurring with moisture from the air. It should also be noted that ground particles were stored in dry, sealed containers, and contain less than 4 wt % water according to thermogravimetric analysis (see Figure S1), so isocyanate reaction due to the presence of water would be very limited. Therefore, it is reasonable to conclude that the particles are capable of reacting as hypothesized, although the reaction kinetics may not be competitive with castor oil, particularly for RH particles. The differences seen between RH and CC particles could be the result of differences in the particle surface area and available −OH groups. However, this analysis does not inform the degree to which particles can participate in the polymerization reaction when mixed with castor oil. As a result, we are also unable to separate the effect of particles from the cross-linking density within the polymer matrix. Many factors, such as temperature, could influence the particle/oil reaction kinetics under foam synthesis conditions.

Gel permeation chromatography was used to study the prepolymer growth as well as indirectly gauge the participation of biofiller particles in the prepolymer reaction. As seen in Figure 3, all prepolymer samples still contain some residual unreacted castor oil (elution at approximately 15 min). Given that the purpose of the prepolymerization step is not to completely react the castor oil but to better balance the reaction in the later foaming step, this residual peak is not concerning. Oligomer species are also present with at least two distinguishable peaks (approximately 14 and 13.6 min). These oligomer species are expected to be mostly linear at this stage due to the limited degree of polymerization. When biofillers are included, the peak height decreases, suggesting the sample is essentially identical in molecular weight distribution but at a lower concentration. Nonetheless, all samples were prepared at the same concentration and had the same injected volume. The difference in concentration therefore arises from filtering, where any insoluble materials (i.e., biofiller particles) were removed. If the biofillers were completely inert, it would be expected that the decrease in the soluble polymer concentration would correspond to the mass of the particles alone. Decreases greater than that amount would indicate that castor oil oligomer species attached to the particles are also removed during filtering. When comparing the rice hull and coffee chaff, the results are fairly similar to 30% RH and 30% CC leading to decreases in peak area of about 27 and 37%, respectively. Since the decrease in peak area for RH is comparable to the particle weight % alone, these results suggest that the RH particles are not participating significantly in the reaction despite the earlier FT-IR results confirming that RH is capable of reacting. The kinetics of the reaction with RH particles may not be fast enough to compete with that of castor oil. In comparison, the decrease in concentration in the CC sample indicates that the particles have participated in the reaction. The apparent higher reactivity of the CC particles could be due to higher surface area or differences in molecular structure leading to more available hydroxyl groups and/or faster reaction kinetics (observed in Figure 2d). It is therefore important to characterize the particle size and shape properties to better understand the potential differences in reactivity.

Figure 4 displays the particle shape and size distributions, including the fine rice hull filler. Based on average values and the shift of the "fines" tails on the left-hand side of Figure 4d, it

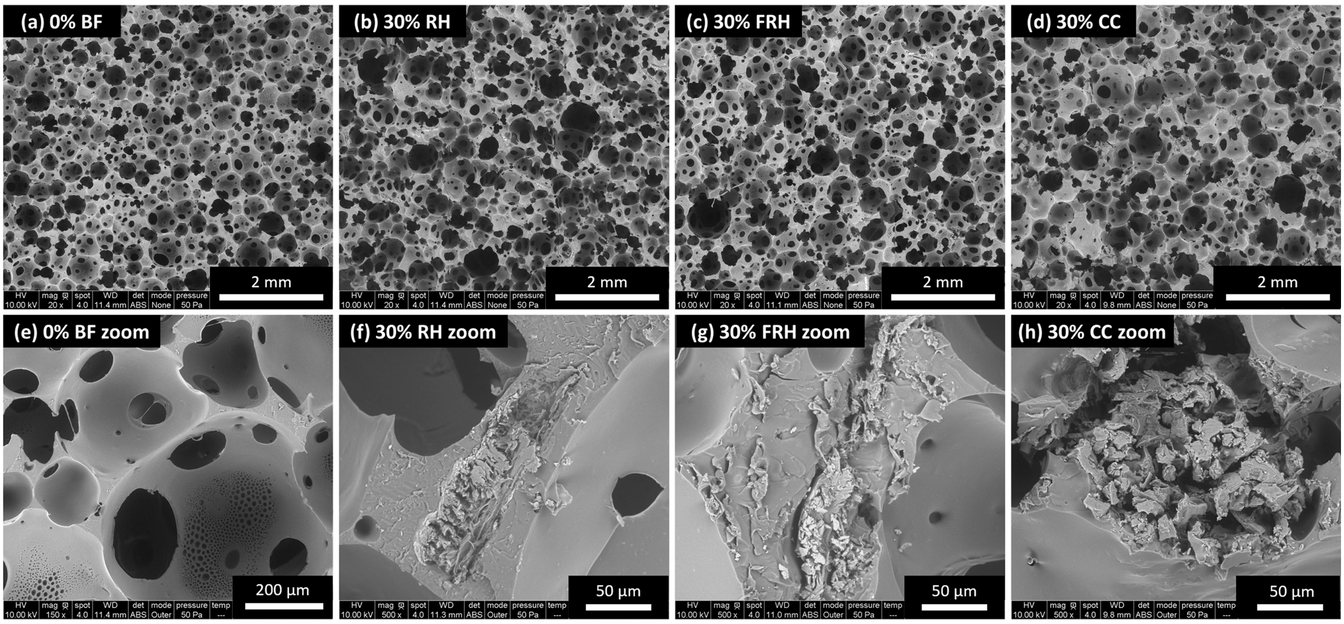

Figure 5. Representative SEM images of foam samples with (a) 0% biofiller, (b) 30% rice hull, (c) 30% fine rice hull, and (d) 30% coffee chaff. (e–g, h) Close-up images from the section of the same samples shown in (a–c) and (d), respectively. (f–h) Images focusing on regions containing visible biofiller particles.

is clear that the CC particles are smallest overall, followed by FRH, and then RH. Interestingly, all three fillers have overlapping "coarse" tails suggesting roughly the same number of very large particles in all distributions. Though some of these may truly be large individual particles, it is likely (particularly for FRH) that these are agglomerates of smaller particles. This could have some important implications for how these particles behave within the polyurethane matrix during expansion and polymerization. If particles are prone to agglomeration when mixed with castor oil, the reactivity of the particles would be reduced due to less available surface area and a continuous particle network with the foam cell walls may not be formed. If particles are well dispersed, then the true size distributions would be shifted left relative to the curves shown in Figure 4d.

Particle shape can give additional information about how particles could potentially agglomerate. The results of the particle shape analysis show FRH particles are more compact than both RH and CC particles, therefore implying a difference in flow and agglomeration behavior that could be expected. Figure 4a–c shows shape maps comparing elliptical form factor (EFF) and aspect ratio (AR) in both number and volume distribution. AR is a measure of elongation, with a value lower than 1 corresponding to a particle that is longer in one direction. EFF is a measure of particle tortuosity. An EFF close to 1 indicates the particle has a relatively smooth, regular shape with minimal surface area. An EFF much lower than 1 indicates that the particle has an irregular shape with a high surface area. Looking only at the number distribution, both CC and RH have very similar profiles. FRH has slightly lower AR and higher EFF on average in comparison, meaning the FRH particles are more smooth and needle-like. In the volume distributions, however, "extra" peaks appear, which are not present in the number distribution plots. These peaks could be attributed both to the presence of large individual particles which account for a significant volume percentage as well as potential particle agglomerates resulting from electrostatic forces. The difference between FRH and the other two fillers is even more apparent in the volume distribution, suggesting the FRH particles are overall more compact and may be less prone to agglomeration.

The foam structure and distribution of biofiller particles within that structure play a critical role in foam performance, though from SEM analysis, few differences were seen between foam structures regardless of particle type and loading. The castor oil foams created in this study have an open cell structure as shown in Figure 5. Cell size in the formulation without biofiller was about 350 μm, on average. As seen in Figure 5b–d, cell size distribution appears to increase slightly when biofiller particles were introduced, though the change is not statistically significant. There is also no noticeable change in the cell wall or strut thickness. Though the structures are not quantifiably different based on the SEM image analysis, visual observation suggests that biofiller particles cause the foam structure to become slightly more "disorganized". More detailed cell size information is provided in the Supporting Information (Figure S3). In general, however, SEM analysis is limited and requires samples to be cut to reveal the internal structures. To that end, there is ongoing work utilizing quantitative and nondestructive imaging techniques, specifically X-ray computational tomography, to better understand the influence of particle type and particle size on foam structure.

Figure 5e,f,h shows examples of biofiller particles embedded within the cell struts. The rice hull particle (Figure 5e) shown appears to be fully compatible with the surrounding polymer matrix. The coffee chaff example (Figure 5f) on the other hand shows clear separation from the polyurethane in some areas. It is possible that this example is an agglomeration of coffee chaff particles, which could explain this instance of poor adhesion. It is also clear from these SEM images, particularly Figure 5f, that the particles have their own internal porosity, creating a layered structure. Another example is provided in the Supporting

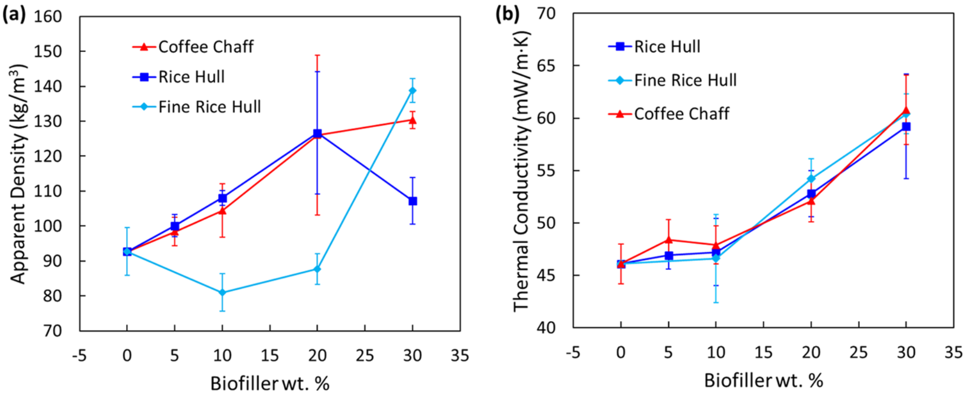

Figure 6. Comparison of rice hull and coffee chaff foam (a) density and (b) thermal conductivity.

Information. This could potentially be a point of mechanical weakness if these layers are prone to peeling apart when bent.

Foam density generally increased with biofiller loading (see Figure 6a), with RH and CC foams showing immediate increases at low loading and FRH foams showing no statistically significant increase until 30%. An increase in density would be expected if the particles had a material density greater than the polyurethane matrix. Biofiller loading also caused an increase in variability, with the 20% RH and CC formulations having standard deviations over twice as broad as the 0% biofiller formulation. The 30% RH formulation is an outlier in the overall trend with a significant decrease in density, while the coffee chaff foams continue to increase. One source of this variation could come from the particles themselves and how they are distributed within the foam. At higher concentrations, the particles may be more prone to form agglomerates[40,41] which could be heavy enough to sink during the early stages of the foaming reaction, leading to a lower concentration of particles in the center of the foam sample. Another possibility is that the increased viscosity caused by the higher particle concentration allowed large bubbles introduced during mixing to remain trapped inside the foam. The FRH formulations also do not directly follow the general trend seen in the other formulations. Both 10 and 20% FRH have a lower density than the 0% biofiller foam, though the differences are not statistically significant. FRH foams experience a significant density increase only when loading reaches 30%.

Figure 6b displays foam thermal conductivity, which has been shown in previous studies to generally be closely correlated with foam density.[42] Indeed, the same general upward trend is seen in thermal conductivity as was observed in foam density. However, in all samples, thermal conductivity did not significantly increase until a biofiller loading of 20 wt %, suggesting that density is not the only determining factor. Given that these foams are composites, it is unsurprising that the particles might have a significant influence over thermal properties. The increasing thermal conductivities are partially an artifact of the biofiller particles, enabling easier heat transfer than the surrounding polymer matrix. Furthermore, the lag in thermal conductivity increase compared to density could signal the formation of interconnected particle networks at sufficiently high concentrations (seemingly 20 wt %). Future inspection of foam structure through nondestructive methods such as X-ray tomography may provide evidence to support this theory. Another factor which could lead to rising thermal conductivity values is the open cell structure of these foams.[43] In general, the thermal conductivity results also reveal that there is not a statistically significant difference among the biofiller types. This suggests that despite differences in particle size and shape distribution, the addition of biofillers will have a consistent and predictable impact on thermal properties.

Mechanical testing was conducted to determine the foam compression strength and fatigue behavior. Figure 7 displays the compression modulus data for all foam formulations including a formulation with a 1.0 NCO index. All other formulations have a 0.75 NCO index. Given that a primary reason for incorporating biofiller particles was to achieve rigidity competitive with higher isocyanate foams, the 1.0 NCO index formulation provides an important point of comparison. Impressively, the 20% CC formulation achieved a modulus competitive with the 1.0 NCO index foam. A clear trend did not form in the RH and CC data, due in part to the high variability seen across all CC and RH foams. The RH foams appear to have an increasing trend in compression modulus until the modulus decreases at 30%. The compression modulus in the CC foams appears to fluctuate, with a large dip occurring at 10%. The cause of this outlier is currently unknown and it should be noted that multiple factors beyond formulation, including laboratory temperature, humidity, and component batches (e.g., batches of coffee chaff ground on different days), may impact final outcomes. SEM images

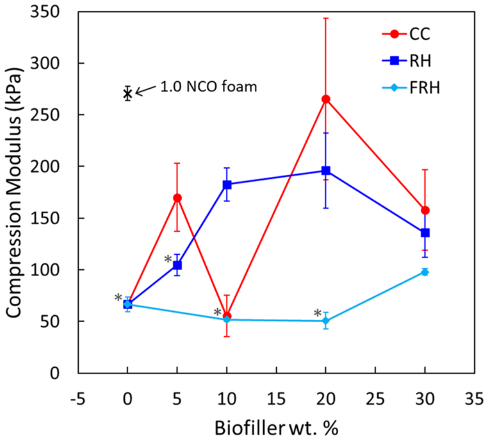

Figure 7. Foam compression modulus as a function of biofiller weight percent. Points marked with asterisks indicate that there was no statistically significant difference from the 0% biofiller 0.75 NCO index foam. A point indicating the modulus of a 0% biofiller 1.0 NCO index foam is shown for an additional comparison.

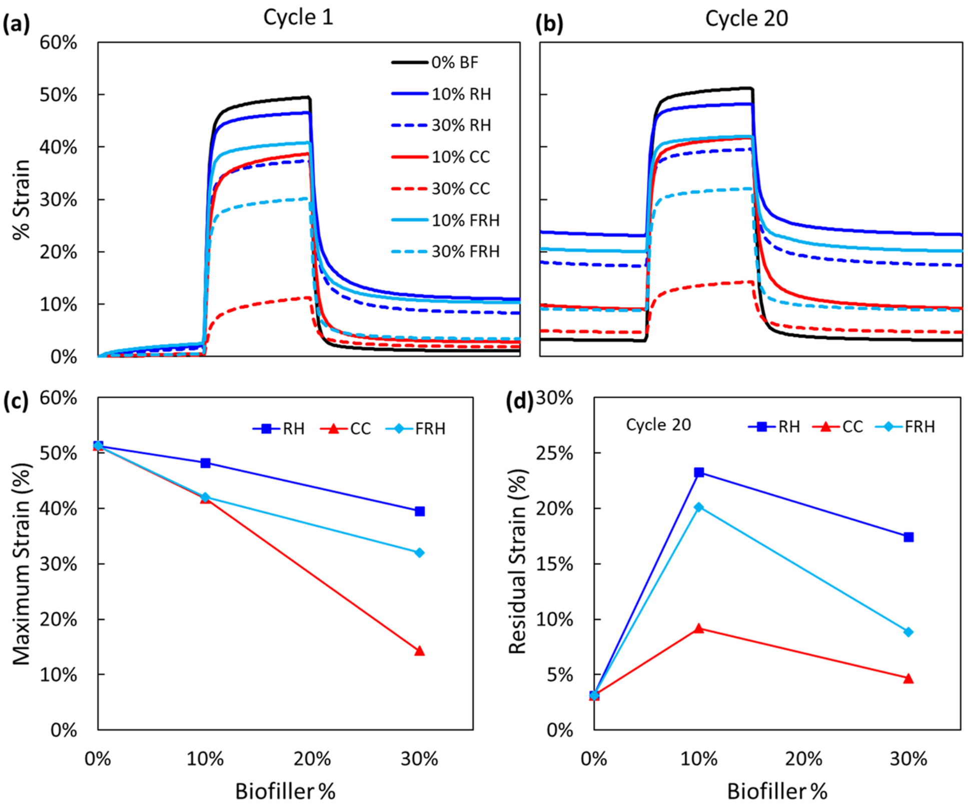

Figure 8. Cyclic creep recovery from compressing samples with cycles of 1000 mN applied force. Strain data during (a) cycle 1 and (b) cycle 20, (c) maximum strain achieved across all cycles, and (d) residual permanent strain following cycle 20.

showed that the 10% CC foam did not deviate significantly in structure compared to other biofiller foams. The 10% CC foam also did not deviate from trends seen in thermal conductivity and density data. If this outlier is disregarded, the compression modulus of CC foams follows the same trend as RH foams. Due in large part to the high variability observed in the RH and CC foams, the finer rice hull grind was prepared and tested.

The results in Figure 7 show that FRH foams drastically improved consistency. However, the compression modulus did not increase until a loading of 30% was reached, which correlates with the density data. In fact, at 10 and 20%, the FRH foam compression modulus was slightly lower than the 0% biofiller foam. One possible explanation for this is that the FRH particles still disrupt the foam cell structure homogeneity but do not provide any reinforcement as a result of the particles being unable to form a network. ImageJ measurements of images seen in Figure 5 showed that 10% RH loading led to an increase in average cell size from 350 to 387 μm (not statistically significant). In general, the presence of biofiller does appear to slightly increase cell size distribution and reduce homogeneity. There are several potential mechanisms through which biofiller particles influence foam structure and subsequent mechanical performance. First, when the particle concentration is low RH and CC particles can already provide reinforcement. This suggests that very coarse particles may provide reinforcement on their own, particularly when the particle−polymer interface has strong adhesion. As the concentration of particles increases, the mechanical performance also increases. One possibility is through mechanical reinforcement with a well-dispersed particle network. When particle concentration is increased to 30 wt %, large aggregates start to form and particle−particle interfaces may be more susceptible to slipping, leading to the reduced moduli seen in RH and CC foams. In addition, particle aggregates within cell walls could account for reduced homogeneity in foam cell structure, which results in large error bars. More importantly, the takeaways from the FRH compression modulus data are that (1) up to 20% of a fine filler can be added without significantly altering mechanical properties making it possible to increase biobased content and reduce the cost of a flexible foam, and (2) there is a significant increase in modulus at 30% weight percent loading, meaning a more rigid foam can still be achieved with a more reliable formulation.

Foam fatigue was tested through cyclic creep recovery. Foams containing biofillers all had increased permanent strain, although fatigue was reduced in the FRH foam compared to the RH foam (Figure 8). The same stress was applied to all samples, which is why the maximum strain changed for each sample. In all formulations, a similar creep rate is observed. Permanent residual strain, on the other hand, depends heavily on the presence of biofiller particles. The sample containing 0% biofiller has less than 5% permanent residual strain after 20 cycles despite experiencing the highest maximum strain out of all of the samples. In other words, the 0% biofiller formulation is both flexible and durable. In comparison, the 10% RH formulation has a permanent strain of about 10% after just the first cycle and about 24% after the 20th cycle. The durability of the biofiller foams is reduced, possibly due to particle delamination or pullout from the polymer when bent, similar to what is observed in Figure 5h. Additionally, it may be possible for the biofiller particles to experience brittle fracture, thereby reducing the ability of the polymer to retain its original shape. Further examination of the foam samples post cyclic

https://doi.org/10.1021/acsapm.3c01536

stress testing would be needed to identify which mechanisms for permanent deformation are most prevalent.

An important thing to note from Figure 8b,c is that the samples with the lowest maximum strain also have a fairly low permanent strain, implying that particle−polymer separation and/or particle fracture generally do not occur as much at small deformations. Thus, these small deformations are likely attributable to the bending of ligament sections which contain little to no particles. Though there is somewhat of a trade-off between increased compression modulus and foam fatigue, future studies of the local fracturing behavior after cyclic applied stress could reveal possible ways to improve the composite properties. The results suggest preparing finer particle grinds can minimize the negative impact on durability. However, particle size analysis (Figure 4d) shows CC particles are only slightly smaller on average compared to FRH, but have substantially lower permanent deformation. Thus, the relationship between particle size and foam durability is not necessarily linear, and/or particle morphology and shape may play an equally significant role. This suggests very coarse particles (>300 μm) may be more prone to mechanical failures such as bending fracture or interface delamination compared to the remaining particle population. Future work should investigate particle morphology and how it may relate to potential failure mechanisms (e.g., particle delamination vs particle fracture) leading to permanent deformation.

■ CONCLUSIONS

The biobased composite polyurethane foams developed in this study show potential as a more sustainable and safer alternative to traditional petroleum-based foam. A wide range of compression moduli were achieved through a series of formulations with varied biofiller selection and loading. Though using biofillers to increase foam rigidity is desirable, the ability to add biofiller without a change in modulus also has benefits. The difference in compression behavior between FRH and RH suggests that there may be a shift in the underlying mechanisms that is highly dependent on particle size/shape distribution and dispersion during the foaming process. FRH particles tend to have less shape "irregularity" compared to both RH and CC, which could influence how the particles flow and pack together. Increased surface area from finer particles could also increase the number of hydroxyl groups available to participate in the polymerization reaction, leading to more interaction between individual particles and the surrounding polymer matrix. Both RH and FRH formulations show increased residual deformation after cyclic applied stress compared to the nonbiofiller counterpart, indicating that regardless of particle size/shape, biofillers can increase foam fatigue.

Future research is needed both to increase the fundamental understanding of particle behavior and to test the feasibility of these biofiller foams in an industrial setting. X-ray computed tomography (XCT) could potentially be used for observing the internal foam structure without damaging the sample. Other biofiller sources such as corn stover may have particle morphologies that are unique. Changing the grinding method could create narrower size and shape distributions to test the effects of those variables. In addition, for commercialization, more testing is needed on how the changes in prepolymer viscosity with biofiller loading may affect mixing and injection into a mold. Reaction speed and curing conditions were also studied further. Castor oil reaction kinetics is limited, so testing formulation modifications to boost reaction and curing speed could be an extremely important step in the successful adoption of these foams into the industry.

■ ASSOCIATED CONTENT

Supporting Information

The Supporting Information is available free of charge at https://pubs.acs.org/doi/10.1021/acsapm.3c01536.

GPC chromatograms of prepolymers and foam cell size data (PDF)

■ AUTHOR INFORMATION

Corresponding Authors

Keith Vorst − *Polymer and Food Protection Consortium and Department of Food Science and Human Nutrition, Iowa State University, Ames, Iowa 50011, United States;* Email: kvorst@iastate.edu

Shan Jiang − *Deparatment of Materials Science and Engineering, Iowa State University, Ames, Iowa 50011, United States; Polymer and Food Protection Consortium, Iowa State University, Ames, Iowa 50011, United States;* orcid.org/0000-0001-8119-9012; Email: sjiang1@iastate.edu

Authors

Rebecca Mort − *Deparatment of Materials Science and Engineering, Iowa State University, Ames, Iowa 50011, United States; Polymer and Food Protection Consortium, Iowa State University, Ames, Iowa 50011, United States;* orcid.org/0009-0009-7818-2696

Erin Peters − *Deparatment of Materials Science and Engineering, Iowa State University, Ames, Iowa 50011, United States*

Elizabeth Griffin − *Deparatment of Materials Science and Engineering, Iowa State University, Ames, Iowa 50011, United States*

Greg Curtzwiler − *Polymer and Food Protection Consortium and Department of Food Science and Human Nutrition, Iowa State University, Ames, Iowa 50011, United States;* orcid.org/0000-0002-4300-7937

Complete contact information is available at: https://pubs.acs.org/10.1021/acsapm.3c01536

Author Contributions

R.M.: Conceptualization, investigation, methodology, sample preparation, data collection, data analysis, writing—original draft. E.P.: Sample preparation, data collection. E.G.: sample preparation, data collection. G.C.: Supervision, conceptualization, writing—review and editing. K.V.: Supervision, conceptualization, funding acquisition, writing—review and editing. S.J.: Supervision, conceptualization, funding acquisition, writing—review and editing.

Funding

This work was supported in part by the Polymer and Food Protection Consortium (PFPC) at Iowa State University under Grant Number GR-025895-00001 DD11523 and the Agricultural and Home Economics Experiment Station (HATCH Project 04202). S.J. and R.M. acknowledge American Chemical Society Petroleum Research Fund under grant no. 60264-DNI7 and Biobased Products Funding support from Iowa State University under grant no. GR-026097-00001.

Notes

The authors declare the following competing financial interest(s): Keith Vorst and Greg Curtzwiler are listed as inventors under a patent related to this research. The patent is owned by Iowa State University.

■ ACKNOWLEDGMENTS

Special thanks go to Dr. Paul Mort at Purdue University, Materials Science and Engineering, for granting access to the Solidsizer equipment used for particle size and shape characterization and for advising on data presentation.

■ REFERENCES

(1) Tarlo, S. M.; Banks, D.; Liss, G.; Broder, I. Outcome determinants for isocyanate induced occupational asthma among compensation claimants. *Occup. Environ. Med.* **1997**, *54*, 756−761.

(2) Lee, S. M.; Koh, D. Lessons from an isocyanate tragedy. *Singapore Med. J.* **2008**, *49* (5), 372−374.

(3) Liang, C.; Gracida-Alvarez, U. R.; Gallant, E. T.; Gillis, P. A.; Margues, Y. A.; Abramo, G. P.; Hawkins, T. R.; Dunn, J. B. Material Flows of Polyurethane in the United States. *Environ. Sci. Technol.* **2021**, *55* (20), 14215−14224.

(4) Geyer, R.; Jambeck, J. R.; Law, K. L. Production, use, and fate of all plastics ever made. *Sci. Adv.* **2017**, *3* (7), No. e1700782, DOI: 10.1126/sciadv.1700782.

(5) Barnes, D. K. A.; Galgani, F.; Thompson, R. C.; Barlaz, M. Accumulation and fragmentation of plastic debris in global environments. *Philos. Trans. R. Soc., B* **2009**, *364* (1526), 1985−1998, DOI: 10.1098/rstb.2008.0205.

(6) Kirpluks, M.; Kalnbunde, D.; Benes, H.; Cabulis, U. Natural oil based highly functional polyols as feedstock for rigid polyurethane foam thermal insulation. *Ind. Crops Prod.* **2018**, *122*, 627−636.

(7) Desroches, M.; Escouvois, M.; Auvergne, R.; Caillol, S.; Boutevin, B. From Vegetable Oils to Polyurethanes: Synthetic Routes to Polyols and Main Industrial Products. *Polym. Rev.* **2012**, *52* (1), 38−79.

(8) Ivey, A.; Talbert, J.; Evangelista, R.; Vorst, K.; Curtzwiler, G. Influence of a hydrocarbon side chain on the performance of Physaria fendleri-Castor oil polyurethane packaging adhesives. *Cleaner Eng. Technol.* **2021**, *4*, No. 100216.

(9) Wai, P. T.; Jiang, P.; Shen, Y.; Zhang, P.; Gu, Q.; Leng, Y. Catalytic developments in the epoxidation of vegetable oils and the analysis methods of epoxidized products. *RSC Adv.* **2019**, *9* (65), 38119−38136.

(10) Danov, S. M.; Kazantsev, O. A.; Esipovich, A. L.; Belousov, A. S.; Rogozhin, A. E.; Kanakov, E. A. Recent advances in the field of selective epoxidation of vegetable oils and their derivatives: A review and perspective. *Catal.: Sci. Technol.* **2017**, *7* (17), 3659−3675.

(11) Sharma, C.; Kumar, S.; Raman Unni, A.; Aswal, V. K.; Rath, S. K.; Harikrishnan, G. Foam stability and polymer phase morphology of flexible polyurethane foams synthesized from castor oil. *J. Appl. Polym. Sci.* **2014**, *131* (17), No. 40668, DOI: 10.1002/app.40668.

(12) Zhang, W.; Deng, H.; Xia, L.; Shen, L.; Zhang, C.; Lu, Q.; Sun, S. Semi-interpenetrating polymer networks prepared from castor oil-based waterborne polyurethanes and carboxymethyl chitosan. *Carbohydr. Polym.* **2021**, *256*, No. 117507.

(13) Tian, H.; Li, Z.; Lu, P.; Wang, Y.; Jia, C.; Wang, H.; Liu, Z.; Zhang, M. Starch and castor oil mutually modified, cross-linked polyurethane for improving the controlled release of urea. *Carbohydr. Polym.* **2021**, *251*, No. 117060.

(14) Al-Moameri, H.; Ghoreishi, R.; Zhao, Y.; Suppes, G. J. Impact of the maximum foam reaction temperature on reducing foam shrinkage. *RSC Adv.* **2015**, *5*, 17171−17178.

(15) Lee, J. H.; Kim, S. H.; Oh, K. W. Bio-based polyurethane foams with castor oil based multifunctional polyols for improved compressive properties. *Polymers* **2021**, *13* (4), 576.

(16) Akindoyo, J. O.; Beg, M. D. H.; Ghazali, S.; Islam, M. R.; Jeyaratnam, N.; Yuvaraj, A. R. Polyurethane types, synthesis and applications - a review. *RSC Adv.* **2016**, *6*, 114453−114482.

(17) Ghasemlou, M.; Daver, F.; Ivanova, E. P.; Adhikari, B. Bio-based routes to synthesize cyclic carbonates ad polyamines precursors of non-isocyanate polyurethanes: a review. *Eur. Polym. J.* **2019**, *118*, 668−684.

(18) El Khezraji, S.; Benyoucef, H.; Belachemi, L.; Lopez Manchado, M. A.; Verdejo, R.; Lahcini, M. Recent progress of non-isocyanate polyurethane foam and their challenges. *Polymers* **2023**, *15* (2), 254.

(19) Tu, Y.-C.; Fan, H.; Suppes, G. J.; Hsieh, F.-H. Physical properties of water-blown rigid polyurethane foams containing epoxidized soybean oil in different isocyanate indices. *J. Appl. Polym. Sci.* **2009**, *114* (5), 2577−2583, DOI: 10.1002/app.30430.

(20) Nik Pauzi, N. N. P.; Majid, R.; Dzulkifli, M. H.; Yahya, M. Y. Development of rigid bio-based polyurethane foam reinforced with nanoclay. *Composites, Part B* **2014**, *67*, 521−526.

(21) Zhang, S.; Xiang, A.; Tian, H.; Rajulu, A. V. Water-Blown Castor Oil-Based Polyurethane Foams with Soy Protein as a Reactive Reinforcing Filler. *J. Polym. Environ.* **2018**, *26* (1), 15−22.

(22) USDA. *Weekly National Rice Summary Mon Oct 24, 2022*; USDA AMS Livestock, Poultry and Grain Market News: Little Rock, AR, 2022 https://www.ams.usda.gov/mnreports/ams_1655.pdf.

(23) Rozman, H. D.; Yeo, Y. S.; Tay, G. S.; Abubakar, A. The mechanical and physical properties of polyurethane composites based on rice husk and polyethylene glycol. *Polym. Test.* **2003**, *22*, 617−623.

(24) Ghasemi, S.; Amini, E. N.; Tajvidi, M.; Kiziltas, A.; Mielewski, D. F.; Gardner, D. J. Flexible polyurethane foams reinforced with organic and inorganic nanofillers. *J. Appl. Polym. Sci.* **2021**, *138* (10), 49983.

(25) Zhang, J.; Hori, N.; Takemura, A. Reinforcement of agricultural wastes liquified polyols based polyurethane foams by agricultural wastes particles. *J. Appl. Polym. Sci.* **2021**, *138*, No. 50583.

(26) Mort, R.; Peters, E.; Curtzwiler, G.; Jiang, S.; Vorst, K. Biofillers improved compression modulus of extruded PLA foams. *Sustainability* **2022**, *14* (9), 5521.

(27) Tessema, A.; Zhao, D.; Moll, J.; Xu, S.; Yang, R.; Li, C.; Kumar, S. K.; Kidane, A. Effect of filler loading, geometry, dispersion and temperature on thermal conductivity of polymer nanocomposites. *Polym. Test.* **2017**, *57*, 101−106.

(28) Al-Saleh, M. H.; Sundararaj, U. Review of the mechanical properties of carbon nanofiber/polymer composites. *Composites, Part A* **2011**, *42* (12), 2126−2142.

(29) ASTM. *D3574−17 Standard Test Methods for Flexible Cellular Materials - Slab, Bonded, and Molded Urethane Foams*; ASTM International, West Conshocken, PA, 2017.

(30) Mort, R.; Cecon, V. S.; Mort, P.; McInturff, K.; Jiang, S.; Vorst, K.; Curtzwiler, G. Sustainable composites using landfill bound materials. *Front. Mater.* **2022**, *9*, No. 849955.

(31) Milijkovic, M. Relative Reactivity of Hydroxyl Groups in Monosaccharides. In *Carbohydrates*; Springer, 2010; pp 113−142.

(32) Listemann, M. L.; Savoca, A. C.; Wressell, A. L.; Lassila, K. R.; Klotz, H. C.; Johnson, G. L.*Polyurethane World Congress* 1993, pp 595−608.

(33) Anejna, A. Structure-property Relationships of Flexibly Polyurethane Foams; Virginia Polytechnic Institute and State University, ProQuest Dissertations and Theses Global, 2002.

(34) Woods, G. *ICI Polyurethanes Book*, 1990.

(35) Ang, T. N.; Hgoh, G. C.; Chua, A. S. M.; Lee, M. G. Eludication of the effect of ionic liquid pretreatment on rice husk via structural analysis. *Biotechnol. Biofuels* **2012**, *5*, No. 67, DOI: 10.1186/1754-6834-5-67.

(36) Socrates, G. *Infrared and Raman Characteristic Group Frequencies: Tables and Charts*; John Wiley & Sons, LTD, 2001.

(37) Zhuang, J.; Li, M.; Pu, Y.; Ragauskas, A. J.; Yoo, C. G. Observation of potential contaminants in processed biomass using Fourier transform infrared spectroscopy. *Appl. Sci.* **2020**, *10* (12), 4345.

(38) Lazzari, L. K.; Zimmermann, M. V. G.; Perondi, D.; Zampieri, V. B.; Zattera, A. J.; Santana, R. M. C. Production of carbon foams from rice husk. *Mater. Res.* **2019**, *22*, No. 0427.

(39) Madra, H.; Tantekin-Ersolmaz, S. B.; Guner, F. S. Monitoring of oil-based polyurethane synthesis by FTIR-ATR. *Polym. Test.* **2009**, *28* (7), 773−779.

(40) Mora, C. F.; Kwan, A. K. H.; Chan, H. C. Particle size distribution analysis of coarse aggregate using digital image processing. *Cem. Concr. Res.* **1998**, *28* (6), 921−932.

(41) Cepuritis, R.; Garboczi, E. J.; Ferraris, C. F.; Jacobsen, S.; Sorensen, B. E. Measurement of particle size distribution and specific surface area for crushed concrete aggregate fines. *Adv. Powder Technol.* **2017**, *28* (3), 706−720.

(42) Mort, R.; Vorst, K.; Curtzwiler, G.; Jiang, S. Biobased foams for thermal insulation: material selection, processing, modelling, and performance. *RSC Adv.* **2021**, *11*, 4375−4394.

(43) Van De Walle, W.; Claes, S.; Janssen, H. Implementation and validation of a 3D image-based prediction model for the thermal conductivity of cellular and granular porous building blocks. *Constr. Build. Mater.* **2018**, *182*, 427−440.

https://doi.org/10.1021/acsapm.3c01536